Energy Conversion and Management 80 (2014) 550–560

Contents lists available at ScienceDirect

Energy Conversion and Management

journal homepage: www.elsevier.com/locate/enconman

Parametric study on the performance of double-layered microchannels heat sink

J.M. Wu [a,b,*], J.Y. Zhao [a], K.J. Tseng [a]

[a] EXQUISITUS, Centre for E-City, School of Electrical and Electronic Engineering, Nanyang Technological University, Singapore 639798, Singapore
[b] State Key Laboratory for Strength and Vibration of Mechanical Structures, Xi'an Jiaotong University, Xi'an City, Shaanxi Province 710049, China

ARTICLE INFO

Article history:
Received 17 September 2013
Accepted 11 January 2014
Available online 24 February 2014

Keywords:
Double-layered heat sink
Performance
Parametric study
Numerical simulation

ABSTRACT

Microchannel is one of several high-heat-flux removal techniques being used in electronic cooling. Double-layered microchannel heat sink (DL-MCHS) with counter current flow arrangement is found not only to be able to lower the thermal resistance of the heat sink, but also decrease the maximum temperature and streamwise temperature rise on the base surface compared with single-layered microchannel heat sink (SL-MCHS). The present paper numerically investigated the thermal resistance, pumping power and temperature distribution on the base surface of substrate of DL-MCHS in different microchannel parameters and flow conditions, so as to find the complicated relationship between the overall performance of DL-MCHS and its geometric parameters and flow conditions. The numerical results show that the optimal width ratio of DL-MCHS should be increased when the microchannel aspect ratio is increased. The effectiveness of increasing aspect ratio of microchannels on improving the overall performance of DL-MCHS is dependent on the pumping power provided. DL-MCHS with higher aspect ratio and smaller width ratio is suited to the situation when higher pumping power is provided. Compared with the situation with identical inlet velocity being assigned to the bottom and upper microchannels, adjusting the inlet velocity of upper channels to be smaller than that of bottom channels may result in the improvement of the overall performance of DL-MCHS at a given pumping power, especially when the given pumping power is lower. These strategies could be tried in the real application of DL-MCHS.

1. Introduction

Heat dissipation or generation in micro-electro-mechanical systems (MEMSs), integrated circuit (IC) boards, laser-diode arrays, high-energy mirrors, and other compact products' applications can easily exceed 200 W/cm^2. Microchannel heat sink (MCHS) is one of several high-heat-flux removal techniques being used in electronic cooling. The effectiveness, compactness and low cost are still the basic requirements to MCHS. These requirements can be detailed as lower thermal resistance, uniform temperature distribution and lower maximum temperature on the base surface, lower pressure drop or pumping power, higher compactness and lower fabrication cost. In recent years, the single-layered microchannel heat sink (SL-MCHS), as shown in Fig. 1, has been extensively used in various electronic devices for cooling purpose. Optimization of the geometric size of SL-MCHS is still a hot research topic to improve the overall performance in its real application.

For still growing miniaturization and integration of electronic devices, circuits and whole systems whose power density are continually increasing, SL-MCHS exhibits a large temperature variation in substrate along the streamwise direction, as well as on the base of the heat sinks. Large temperature variation results in thermal stresses in devices and then reduces the electrical performance via electrical–thermal instability, thermal breakdown, etc. Increasing depth or aspect ratio (ratio of depth to width) of microchannel in SL-MCHS can allow more coolant flowing through the microchannels to carry high heat load away. However, aspect ratio of microchannel is a very sensitive parameter to the overall performance and fabrication of heat sink. Firstly, the pressure drop due to flow friction in a microchannel increases dramatically when the channel size shrinks, leading to an increase of pumping power required. Secondly, the difficulties associated with the microfabrication and bulky package of electronic devices also increase when aspect ratio of microchannels is increased. Vafai and Zhu [1] first proposed a conceptual design for double-layered microchannel heat sink (DL-MCHS), as shown in Fig. 2, to allow more coolant flowing through the channels. In Fig. 2, two layers of microchannel heat sink structures are stacked, one atop the other, with coolant

* Corresponding author at: School of Aerospace, Xi'an Jiaotong University, Xi'an City, Shaanxi Province 710049, China. Tel./fax: +86 29 82663401.
E-mail address: wjmxjtu@mail.xjtu.edu.cn (J.M. Wu).

http://dx.doi.org/10.1016/j.enconman.2014.01.014
0196-8904/

Nomenclature

c_p	specific heat capacity (J/kg K m)
h	heat sink total height (μm)
h_{ch}	microchannel depth (μm)
k	thermal conductivity (W/m K)
L	heat sink total length (μm)
N	microchannel number
P	pumping power (W)
q	heat flux of heat sink (W/m^2)
R_{th}	thermal resistance (K/W)
t_b	bottom thickness of substrate (μm)
t_u	middle thickness of substrate (μm)
T	temperature (K)
u	velocity (m/s)
$\dot{V}$	volume flow rate (m^3/s)
W	heat sink total width (μm)
W_{ch}	microchannel width (μm)
W_f	fin width between channels (μm)
x_i	direction coordinates, i = 1,2,3 (m)

Greek symbols

α	aspect ratio
β	width ratio
γ	velocity ratio
Δp	pressure drop (Pa)
ΔT	temperature difference (K)
Φ	viscous dissipation function (1/s^2)
η	dynamic viscosity (N/m^2 s)
ρ	density (kg/m^3)

Subscripts

b	bottom channel
in	inlet
i,j,k	index
max	maximum
s	solid
u	upper channel
w	wall

flows in the opposite direction (counterflow arrangement) in each of the microchannel layers. The following review will show that parallel flow arrangement (coolant flows in the same direction in stacked microchannels) was also suggested in other research. Vafai and Zhu [1]'s results indicated that the upper and bottom layers of the fluid had apparent different temperature difference. At the two ends of the microchannels, there were regions where the outlet coolant temperature for one layer was higher than the temperature of the surrounding substrate cooled by the other coolant layer at its inlet. This implies that heat transfer also occurs from the heated coolant to the substrate around in somewhere, compensating the streamwise temperature rises for the coolant and the substrate through conduction between the two layers. The maximum temperature on the heated surface for DL-MCHS occurs at some position in-between the two ends. This is different from that in a SL-MCHS structure where the maximum temperature occurs at the coolant outlet end. The maximum temperature difference in the streamwise direction in the double-layered structure was greatly decreased compared with that of single-layered one when the pressure drops and other parameters were kept the same for the two structures. Wei and Joshi [2] numerically investigated a heat sink based on a multilayer stack of liquid cooled microchannels with parallel flow arrangement. For a given heat removal capability for the heat sink, the required pumping power for a stack of microchannels was found significantly lower compared to a SL-MCHS, while the required flow rate for a double-layered microchannel heat sink was slightly lower compared to a SL-MCHS. Wei et al. [3] experimentally measured and numerically simulated the effects of coolant flow direction (counter flow or parallel flow), flow rate allocation among layers, and non-uniform heating on the thermal performance of DL-MCHS. Excellent overall cooling performance (thermal resistance was low to 0.09 K/W cm^2) had been shown for the stacked microchannel heat sink in their experiments. It had also been identified that over the tested flow rate range, counterflow arrangement provided better temperature uniformity, while parallel flow had the best performance in reducing the peak temperature when flow rate was low. It was indicated that the flow ratio between the top and bottom layers can be customized to achieve both low pumping power and superior thermal performance. Levac et al. [4] conducted a three-dimensional

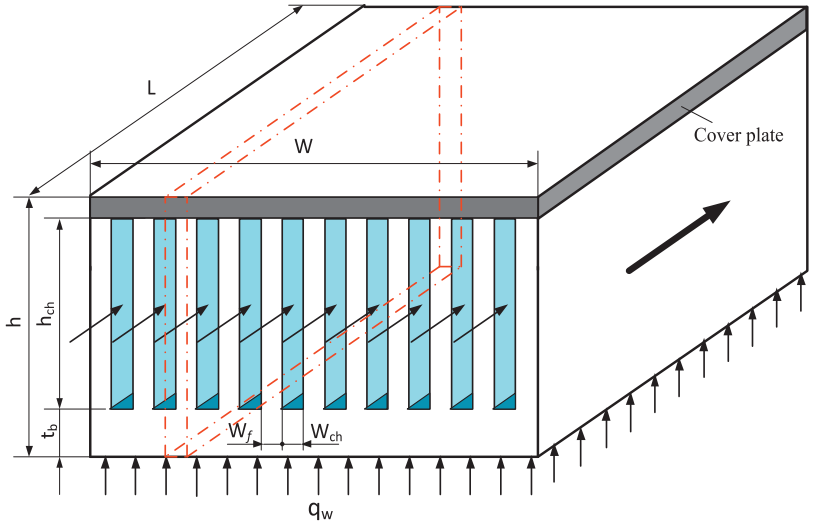

Fig. 1. Schematic of SL-MCHS.

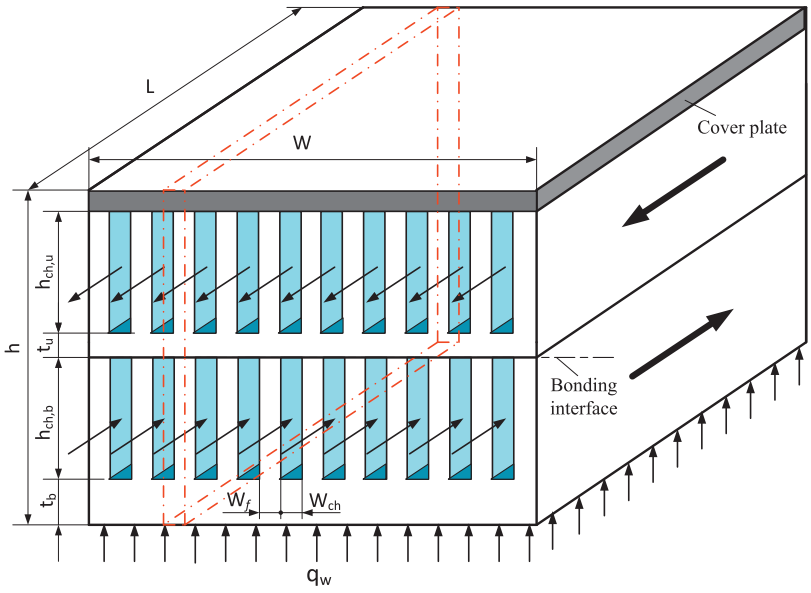

Fig. 2. Schematic of DL-MCHS.

numerical analysis of laminar fluid flow and conjugate heat transfer for single- and double-layered microchannel heat sinks. The effects of Reynolds number, inlet velocity profile, and flow arrangement in the channels (counter flow or parallel flow) on the overall thermal resistance, pumping power, the maximum temperature difference on the heat-sink heated surface were presented and discussed.

Recently Hung et al. [5–8] published their series theoretical or numerical studies on the effects of the substrate materials, coolants, geometrical configuration and pumping power on the thermal performance of microchannel heat sink. Hung et al. [5]'s results showed that a lower temperature rise was experienced for a DL-MCHS with substrate and coolant of higher conductivity ratio. A coolant with high thermal conductivity and low dynamic viscosity also enhances the heat transfer performance. In their study of geometric parameters effects, the base surface area ($L \times W$) of the heat sink was fixed, and the heights of the bottom and upper microchannels were kept the same. Thus the total height of the heat sink was varied with the changes of channel number, channel aspect ratio or channel width ratio. The results showed that an increase in channel aspect ratio or channel width ratio could reduce the pressure drop of DL-MCHS. The down-and-up trend occurred in the relationship between the total thermal resistance and the channel number, channel aspect ratio or channel width ratio. That means a minimal thermal resistance could be obtained by properly adjusting the geometric parameters of DL-MCHS to their optimal values. Hung et al. [6] used an optimization procedure consisting of a simplified conjugate-gradient method and a three-dimensional fluid flow and heat transfer model to investigate the optimal geometric parameters of a DL-MCHS. In their optimization, the base surface area ($L \times W$) and the total height of the heat sink was fixed, and the height of the bottom microchannels was varied with the changes of channel number, bottom channel aspect ratio or channel width ratio. Accordingly, the height or aspect ratio of the upper channels may also be changed and have different values from those of upper channels. The effects of the channel number N, bottom channel aspect ratio α_b, upper channel aspect ratio α_u, and channel width ratio β on the optimal thermal resistance were examined in this study. The results showed that for a given bottom area (10×10 mm) and heat flux (100 W/cm^2), the optimal (minimum) thermal resistance of the DL-MCHS was found to be about 0.12 °C/m^2 W. The corresponding optimal geometric parameters were $N = 73$, $\beta = 0.50$, $\alpha_b = 3.52$, and, $\alpha_u = 7.21$ under a total pumping power of 0.1 W. Hung et al. [7] constructed three-dimensional models of microchannel heat sinks (MCHSs) with different geometric configurations (such as single-layered- (SL), double-layered- (DL) or tapered-(T)-channels) by an optimization procedure. As in Hung et al. [6], fixed base surface area ($L \times W$) and the total height of the heat sink were taken as design constraints. The aspect ratios of bottom and upper channels for DL-design had different values. The results showed that the optimal T-MCHS design has the lowest value of thermal resistance while the SL-MCHS has the highest one followed by the DL-MCHS with a given pumping power. Unfortunately, the geometric sizes of the heat sinks corresponding to the optimal SL-, DL- and T-channel designs were not presented in this paper. Hung and Yan [8] conducted a three-dimensional analysis to enhance the thermal performance of a DL-MCHS by using nanofluids and varying the geometric parameters. The thermal resistance of heat sink was shown to be sensitive to the type of nanofluid and its particle volume fraction. The Al_2O_3 (1%)–water nanofluid showed an average enhancement in thermal performance over that of pure water of 26%. However, the design's effectiveness declined significantly under high pumping power. As in Hung et al. [5], the heights of the bottom and upper microchannels were kept the same while the total height of the heat sink was varied with the changes of channel number, channel aspect ratio or channel width ratio. The down-and-up trend also occurred in the relationship between the total thermal resistance and the channel number, channel aspect ratio or channel width ratio in the DL-MCHS with nanofluids as coolants.

Xie et al. [9] numerically investigated the laminar heat transfer and pressure loss of a kind of DL-MCHS. The results showed that DL-MCHS not only reduced the pressure drop effectively but also exhibited better thermal characteristics. The parallel-flow layout was found to be better for heat dissipation when the flow rate is low, while the counter-flow layout was better when a high flow rate can be provided.

The above reviews show that the multi-layered microchannel heat sink design exhibits better overall thermal performance than a single-layered one. Multi-layered microchannel heat sink, especially DL-MCHS should have great potential for use as a cooling device in electronic equipment with higher power density, deserving more efforts to carry out deeper research on its optimal

configuration and working conditions. However, to the authors' best knowledge, the research on the thermal performances of DL-MCHS is much less than that of SL-MCHS. As a fact, many efforts have been conducted to analyze the possible optimal structure sizes for single-layered heat sink using theoretical fin efficiency method and/or numerical computation method. It is interesting to note that optimal geometries suggested by these two approaches were seldom similar due to the fact that a number of assumptions and different constraints are always applied to the different optimization work [10]. So far, numerical computation method is thought to be more accurate due to less assumptions being used in optimization work than theoretical fin efficiency method.

Thus, the present paper will numerically investigates the thermal resistance, pumping power and temperature distribution on the base surface of substrate of double-layered silica heat sinks in counter-flow arrangement. The effect of different geometric parameters and flow conditions of microchannel are evaluated, so as to find the complicated relationship between the overall performance of double-layered heat sink and its geometric parameters and flow conditions. It should be noted that optimization in the previously published work [5–8] was often conducted under the condition of fixed pumping power. That means an empirical expression between the pumping power and the inlet velocity, geometric sizes of microchannel has to be used to calculate the inlet velocity of microchannel, a necessary boundary condition for numerical simulation. An uncertainty must exist in the selected empirical expression. In our simulation, the empirical expression is not needed any more. The relationship between the pumping power and the inlet velocity, geometric sizes of microchannel is gained by solving the governing equations during simulation. The constraint conditions of fixed bulk sizes (including length, width and height) and heat removal (heat flux on the base surface) are applied to the double-layered heat sink simulated in the present paper. And the depths of the bottom and upper channels are kept the same. Therefore, the constraint conditions used in the present paper are different from those in open articles in some manner.

2. The design of geometric configuration and flow conditions of DL-MCHS for computation

As stated above, the present study keeps the bulk sizes ($L \times W \times h$) and heat removal capacity of DL-MCHS as constants. The depths of upper and bottom microchannels are the same and unchanged ($h_{ch,u} = h_{ch,b}$), the width (W_{ch}) and number (N) of microchannels, the fin width (W_f) are changed. Thus the aspect ratio ($\alpha = h_{ch,b}/W_{ch}$) of microchannels and the channel width ratio ($\beta = W_f/W_{ch}$) of the heat sink vary accordingly. The thermal performance of DL-MCHS with different channel aspect ratio and width ratio is numerically investigated and compared in the present paper. It is known that the flow rate in the microchannels seriously influences the convective thermal resistance and pressure drop of microchannels. Therefore, the present study also tries to assign different inlet velocities to the upper and bottom microchannels to investigate the effect of velocity ratio ($\gamma = u_{in,u}/u_{in,b}$) on the thermal performance of DL-MCHS. For these purposes, the geometric parameters and flow conditions of DL-MCHS for computation are listed in Table 1. The heat flux of q_w is fixed at 200 W/cm^2 which is about double of the normal level of heat generation rate of modern electronic equipment. The heated surface area for all cases is 1 cm $\times$ 1 cm as referred to per unit heating area of heat sink. The height (700 for SL- /740 μm for DL-) of the heat sink is selected according to the modest height of heat sink between 450 and 900 μm as shown in most literature.

To valid the superiority of DL-MCHS, the performance of a SL-MCHS with channel depth of h_{ch} ($=h_{ch,u} + h_{ch,b}$) is also simulated. The total height of the SL-MCHS is less than that of DL-MCHS due to omission of t_u shown in Fig. 2. The substrate material of the all cases is supposed to be silicon whose thermo-physical properties are shown in Table 2. The working fluid of all cases is water whose thermal conductivity and dynamic viscosity are temperature-dependent.

3. Models used in the simulation

3.1. Governing equations and models

A 3D conjugate heat transfer model is used to consider the conjugated heat transfer among the heat sink material and coolant. The flow in microchannel is assumed to be steady and laminar by controlling the maximum inlet Reynolds number below 600. The governing equations include equations of mass conservation, momentum conservation and energy conservation in coolant region and energy conservation in solid substrate region. It should be noted that the viscous dissipation term should be included in the energy equation in coolant region.Mass conservation:

$$\frac{\partial(\rho u_i)}{\partial x_i} = 0 \tag{1}$$

Momentum conservation:

$$\frac{\partial(\rho u_k u_i)}{\partial x_k} = -\frac{\partial p}{\partial x_i} + \eta \frac{\partial}{\partial x_k}\left(\frac{\partial u_i}{\partial x_k}\right) \tag{2}$$

Energy conservation in fluid with consideration of viscous dissipation:

$$\frac{\partial(\rho u_i T)}{\partial x_i} = \frac{\partial}{\partial x_i}\left(\frac{k}{c_p}\frac{\partial T}{\partial x_i}\right) + \frac{\eta}{c_p}\Phi \tag{3}$$

$$\text{where} \quad \Phi = \left(\frac{\partial u_i}{\partial x_j} + \frac{\partial u_j}{\partial x_i}\right)\frac{\partial u_i}{\partial x_j}$$

Here, Φ is the viscous dissipation function.

Energy conservation in solid substrate region:

Table 1
Geometric size of the computed heat sinks and microchannels.

Parameters	SL-MCHS (Fig. 1)	DL-MCHS in counterflow (Fig. 2)							
Microchannel width, W_{ch} (μm)	50	50			70			40	
Fin width between channels, W_f (μm)	50	50	33	25	70	48	36	40	25
Microchannel number	100	100 × 2	120 × 2	133 × 2	71 × 2	84 × 2	94 × 2	153 × 2	125 × 2
Channel depth, h_{ch} (μm)									
$h_{ch,u}$ (μm)	500	250			250			250	
$h_{ch,b}$ (μm)		250			250			250	
Bottom thickness of substrate, t_b (μm)	160	160			160			160	
Middle thickness of substrate, t_u (μm)	/	40			40			40	
Heat sink total height, h (μm)	700	740			740			740	
Heat sink total width, W (μm)	10,000	10,000			10,000			10,000	
Heat sink total length, L (μm)	10,000	10,000			10,000			10,000	

Table 2
Thermo-physical properties of heat sink substrate material.

Material	Density, ρ_s (kg/m^3)	Thermal conductivity, k_s (W/m K)	Specific heat capacity, c_{ps} (J/kg K)
Si	2330	149	712

$$\frac{\partial}{\partial x_i}\left(k_s \frac{\partial T}{\partial x_i}\right) = 0 \tag{4}$$

In this simulation, models of temperature-dependent thermal conductivity and dynamic viscosity of water shown in Eqs. (5) and (6) are integrated into the governing equations. The temperature fields in both fluid and solid regions are obtained simultaneously by conjugate computation of the above equation set with the following boundary conditions.

$$k(T) = -1.079257 + 9.43573 \times 10^{-3}\, T - 1.266071 \times 10^{-5}\, T^2 \tag{5}$$

$$\eta(T) = 2.414 \times 10^{-5} \times 10^{\frac{247.8}{T-140}} \tag{6}$$

3.2. Boundary conditions

Due to the geometric symmetry of the medial microchannels, the regions enclosed by the dashed lines in Figs. 1 and 2 are selected as the computational domains in the following simulation. The computational domain for every case consists vertically of half of a medial microchannel along with half of a fin, as shown in Fig. 3. Corresponding to Fig. 3, the boundary conditions used in the simulation are listed in Table 3.

3.3. Numerical methods and data handling

The software package ANSYS FLUENT 12.0 was used for the computations. To improve the accuracy of the numerical results, the hexahedral mesh is finer in the fluid region and is coarser in solid region. Numerical tests show that a grid system of $600(x) \times 96(y) \times 24(z)$ is fine enough to obtain the grid-independent numerical solution. Such a grid system is adopted in all the simulations of this paper. The convective term is discretized using second-order upwind scheme, while the diffusion term is discretized using QUICK scheme. The substrate region is defined as solid region in which the velocity of 0 is assigned automatically and only heat conduction equation is solved. The coupling between pressure and velocity is implemented by SIMPLEC algorithm. The convergence criterion for the velocity is that the maximum mass residual of the cells divided by the maximum residual of the first 5 iterations is less than 10^{-4}. Our numerical practice found that once the above referenced condition was satisfied the residuals of momentum and energy equations were all less than 10^{-7}.

Based the computed velocity and temperature fields, the following quantities are calculated to compare the numerical results of different cases.

Thermal resistance of heat sink, R_{th} is defined as,

$$R_{th} = \frac{T_{w,max} - T_{in}}{Q} \tag{7}$$

where $T_{w,max}$ is maximum wall temperature of heated surface, K. T_{in} is inlet temperature of coolant, K. Q is the heat flow carried away by coolant, W.

Pumping power of heat sink, P is defined as,

$$P = \Delta p_b \cdot \dot{V}_b + \Delta p_u \cdot \dot{V}_u \tag{8}$$

where Δp is the pressure drop of coolant between microchannels inlet and outlet, Pa. $\dot{V}$ is volume flow rate of coolant in mcrochannels, m^3/s. The subscripts of "b" and "u" represent the bottom and upper channels of DL-MCHS, respectively. That means the total pump power of DL-MCHS should be the sum of the required pump powers to drive the coolant flow in upper and lower microchannels. Naturally, only one term in the right of Eq. (8) is needed for SL-MCHS.

The maximum temperature rise of $\Delta T_{max,s}$ is defined as the temperature difference between maximum and minimum temperature on the heated surface, to reflect the uniformity of temperature distribution of the heat sink.

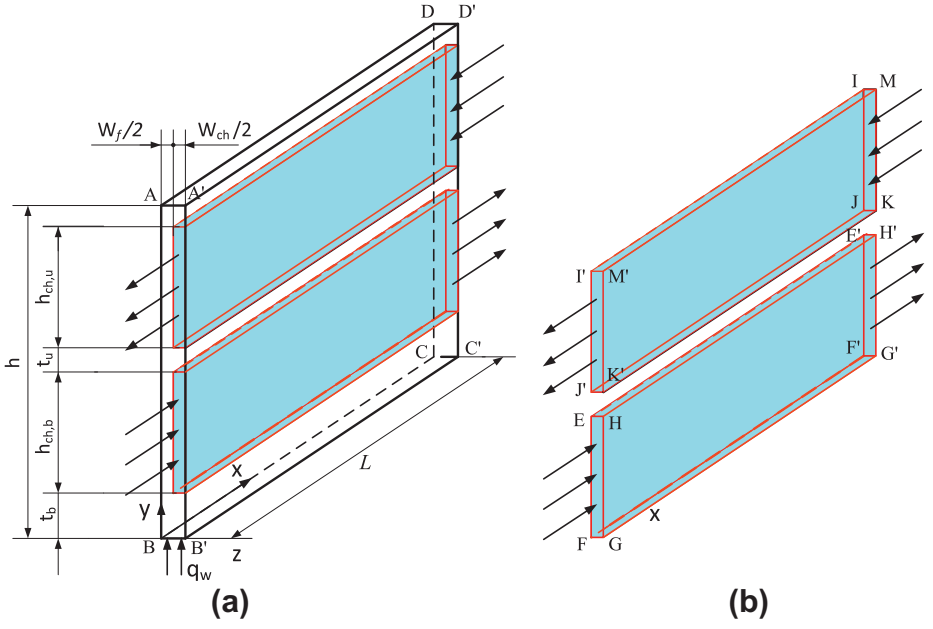

Fig. 3. (a) Schematic of the computational domain of DL-MCHS; (b) extracted upper and bottom channels for labelling vertexes.

3.4. Validation of models and methods

To validate the abovementioned numerical models and methods, pure water flow in the SL-MCHS is simulated first. The simulated temperature differences from the microchannel inlet to outlet as a function of inlet velocity are compared with the theoretical values predicted by Eq. (9). A maximum relative deviation between the numerical results and theoretical predictions in the computed velocity range is less than 1.4%. This validates the effectiveness and reliability of the present numerical models and methods.

$$\Delta T = T_2 - T_1 = \frac{Q}{\dot{m} c_p} \tag{9}$$

where $\dot{m}$ is the mass flow rate of coolant, $= \rho \cdot \dot{V}$, kg/s.

4. Numerical results and discussion

4.1. Comparison of thermal performance between SL-MCHS and DL-MCHS

The performance of a SL-MCHS with channel parameters shown in Table 1 is simulated and compared with that of the DL-MCHS case with the same channel width (W_{ch} = 50 μm), fin width (W_f = 50 μm) and channel number of 2 × 100. For DL-MCHS, identical velocity is always assigned to the upper and bottom channels inlet. Figs. 4–6 compare the performance of SL-MCHS and DL-MCHS along with different inlet velocities. Fig. 4 shows that in lower inlet velocity conditions (about less than 1.2 m/s in these two cases), SL-MCHS has lower thermal resistance than DL-MCHS. While in higher inlet velocity conditions, DL-MCHS provides an obvious reduction of overall thermal resistance over SL-MCHS. Fig. 5 shows that DL-MCHS just brings about a slight increase in pumping power compared with that of SL-MCHS in the same inlet velocity. The increase in pumping power of DL-MCHS is about 5.6% when inlet velocity is of 3.5 m/s. It is found from Fig. 6 that DL-MCHS greatly decreases the maximum temperature rises and improves the uniformity of temperature distribution on the base surface of heat sink. The numerical results show that the maximum temperature on the base surface of DL-MCHS is also decreased about 0.7 K compared with that of SL-MCHS. These benefits are very important to the stability of electronic devices. Fig. 7 shows the relationships of thermal resistance and required pumping power for the SL-MCHS and DL-MCHS. One can find that with given pumping power (larger than 0.1 W), DL-MCHS exhibits lower thermal resistance. Thus, the following work is directing to optimize the overall performance of DL-MCHS by matching the geometric sizes and flow conditions of microchannel with given pumping power, to push its potential practical application in electronic cooling.

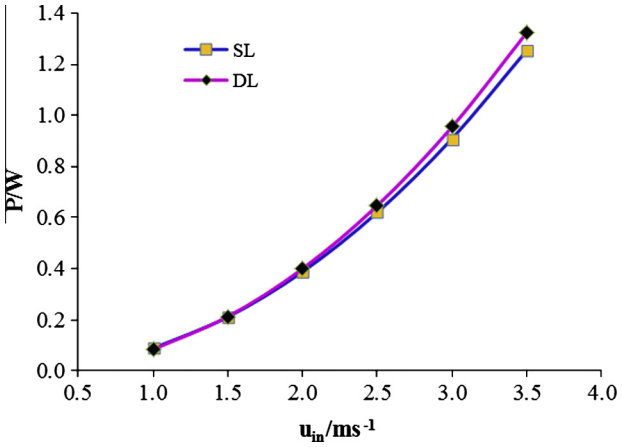

Fig. 5. Comparison of pumping power vs. inlet velocity between SL- and DL-MCHSs.

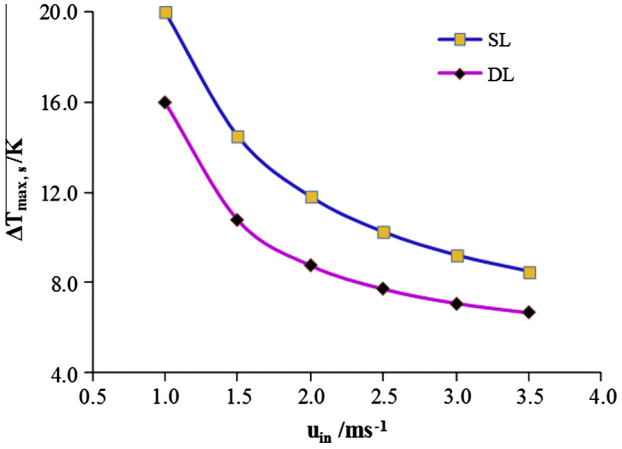

Fig. 6. Comparison of maximum temperature rise vs. inlet velocity between SL- and DL-MCHS.

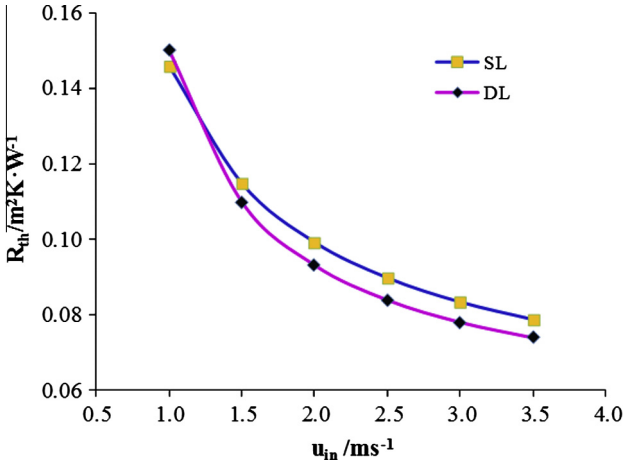

Fig. 4. Comparison of thermal resistance vs. inlet velocity between SL- and DL-MCHSs.

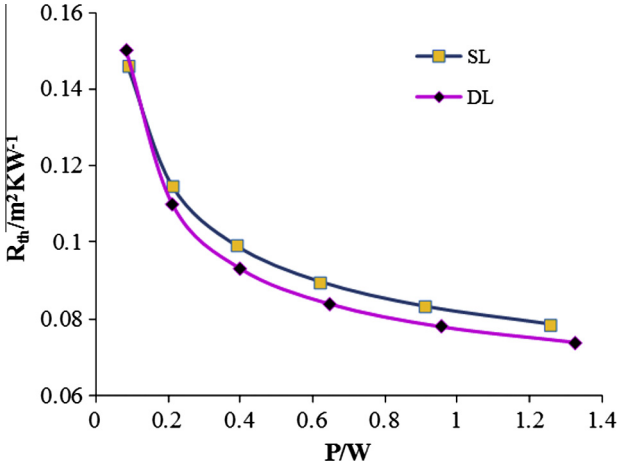

Fig. 7. Comparison of thermal resistance vs. pumping power between SL- and DL-MCHSs.

Table 3
Boundary conditions used in the simulation.

Boundaries	Labelled as	Conditions	Remark
Inlet of microchannel	Surfaces of EFGH and IJKM	Uniform velocity and temperature	Fixed inlet temperature of 300 K is given for every case. The signs of inlet velocities at surfaces of EFGH and IJKM should be opposite for DL-MCHS because of counter-flow arrangement
Outlet of microchannel	Surfaces of E′F′G′H′ and I′J′K′M′	Pressure outlet	
Side boundaries	Surfaces of ABCD and A′B′C′D′	Symmetry	
Base of heat sink	Surface of BB′C′C	No-slip and uniform heat flux	
Upper boundaries	Surface of AA′D′D	No-slip and adiabatic	
Both ends of substrate	Surfaces of ABB′GFEHK′J′M′A′ and DCC′G′F′E′H′KJIMD′	No-slip and adiabatic	

4.2. Effect of channel number (width ratio) of microchannels on the performance of DL-MCHS

For the first step, DL-MCHSs with microchannel widths of 50 and 70 μm are chosen to be investigated. The corresponding upper/lower microchannels aspect ratios of α for these two DL-MCHSs are 5 and 3.57, respectively. For every aspect ratio of DL-MCHS, three microchannel numbers/fin widths are designed, shown in Table 1. Their corresponding width ratios of β are 1.0 (W_f = 50 μm, N = 100), 0.66 (W_f = 33 μm, N = 120) and 0.5 (W_f = 25 - μm, N = 133), respectively for DL-MCHS with channel width of 50 μm, and 1.0 (W_f = 70 μm, N = 71), 0.69 (W_f = 48 μm, N = 84) and 0.51 (W_f = 36 μm, N = 94) for DL-MCHS with channel width of 70 μm, respectively. Thus the cases of "N = 100" and "N = 71" have almost the same width ratios but different aspect ratios, so do the cases of "N = 120" and "N = 84", and cases of "N = 133" and "N = 94".

Figs. 8–10 show the effect of channel number or width ratios on the thermal performance of DL-MCHS with channel width of 50 μm (α = 5.0). One can find from Fig. 8 that in lower inlet velocity condition, the thermal resistance is decreased with increase of channel number (the decrease of width ratio). However, in higher inlet velocity (maybe exceeds 1.8 m/s in this heat sink) the thermal resistance of the case of N = 120 (β = 0.66) is lower than that of the case of N = 133 (β = 0.50), even though not so much. This indicates the increase of channel number (decrease of width ratio) does not always bring about the decrease of thermal resistance of DL-MCHS. However, the pumping power is greatly increased with the increase of channel number because of viscous friction. To compare the gain and cost of increasing channel number, the variation of thermal resistance along with the consumed pumping power is shown in Fig. 9. It is found that at a given pumping power, the case

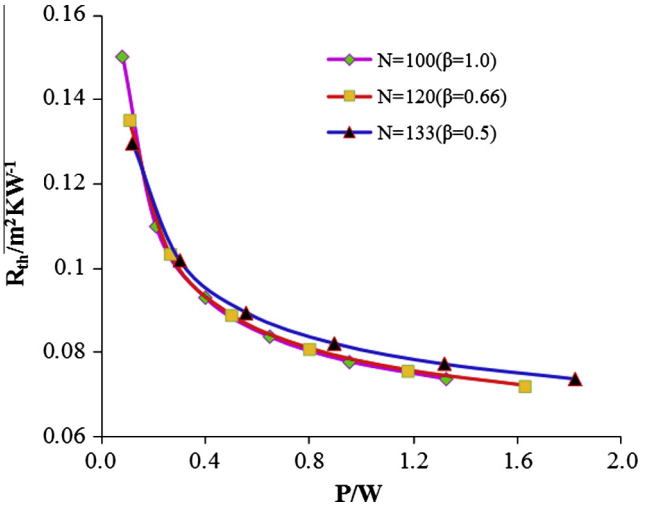

Fig. 9. Comparison of thermal resistance vs. pumping power between the three cases of W_{ch} = 50 μm.

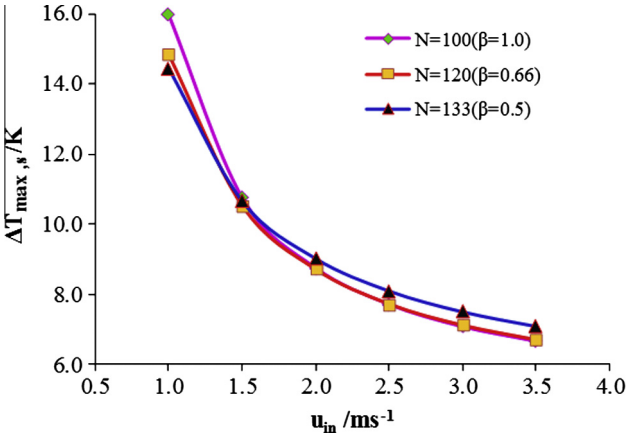

Fig. 10. Comparison of temperature rise vs. inlet velocity between the three cases of W_{ch} = 50 μm.

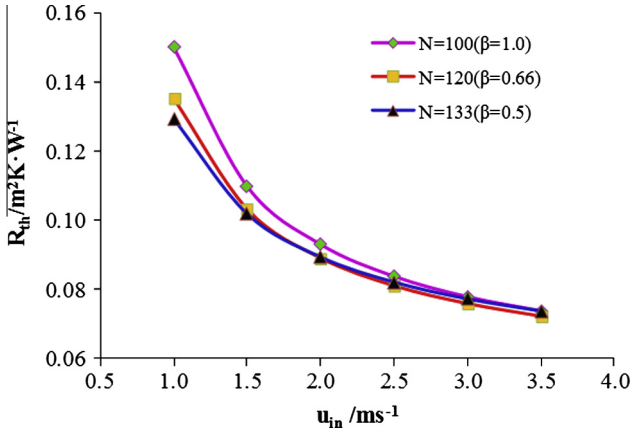

Fig. 8. Comparison of thermal resistance vs. inlet velocity between the three cases of W_{ch} = 50 μm.

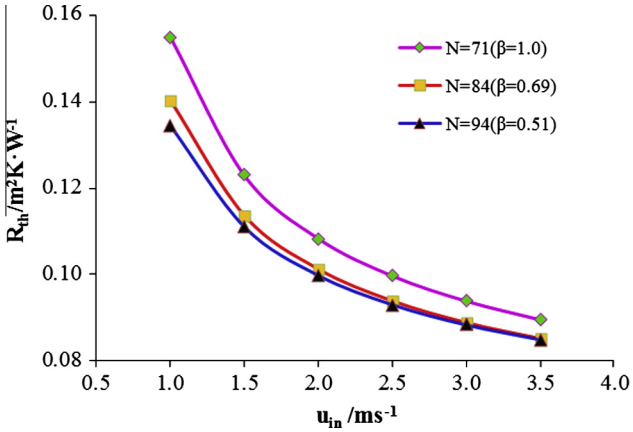

Fig. 11. Comparison of thermal resistance vs. inlet velocity between the three cases of W_{ch} = 70 μm.

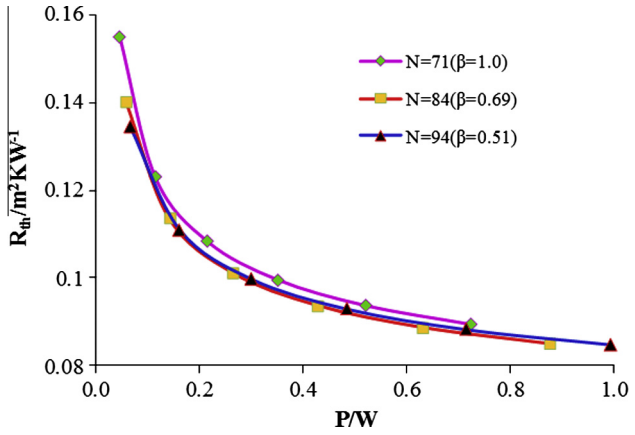

Fig. 12. Comparison of thermal resistance vs. pumping power between the three cases of W_{ch} = 70 μm.

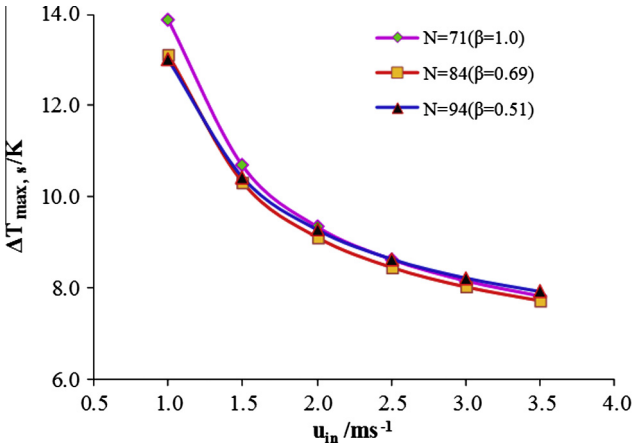

Fig. 13. Comparison of temperature rise vs. inlet velocity between the three cases W_{ch} = 70 μm.

of N = 133 (β = 0.50) exhibits largest thermal resistance in the three cases. Fig. 10 also shows that in lower inlet velocity conditions, the increase of channel number is effective to improve the uniformity of temperature distribution on the base surface of heat sink. However, in higher inlet velocity conditions, the temperature rises of the case of N = 133 (β = 0.5) exceed those of the other two cases. Thus, the design with channel number 120 (β = 0.66) is considered to provide better overall performance of the heat sink with microchannel width of 50 μm (α = 5.0).

Figs. 11–13 show the numerical results of DL-MCHS with microchannel width of 70 μm (α = 3.57). One can find from Fig. 11 that the thermal resistance is decreased with the increase of channel number (decrease of width ratio) in the whole range of computational inlet velocity. However, the decrease of thermal resistance of the case of N = 94 (β = 0.51) is minor compared with that of the case of N = 84 (β = 0.69) when inlet velocity exceeds 2.0 m/s. Again, the pumping power is greatly increased with the increase of channel number. The variation of thermal resistance along with the consumed pumping power for the three cases with channel width of 70 μm is shown in Fig. 12. It is found that with a given pumping power, the case of N = 71 (β = 1.0) exhibits largest thermal resistance while the case of N = 84 (β = 0.69) contributes lowest thermal resistance in higher pumping power. Fig. 13 shows that the case of N = 84 (β = 0.69) provides lowest temperature rise along heated surface in the three cases. Thus, the case with channel number of 84 (β = 0.69) is considered to be able to provide better overall performance of the heat sink with microchannel width of 70 μm (α = 3.57).

The above results show that for DL-MCHS with smaller microchannel width, the optimal width ratio of β is not 0.50, should be around 0.6–0.7 for the above cases. This is not coincident with the results from Hung et al. [6], in which the optimal width ratio of β was concluded as 0.50, and the optimal aspect ratios of bottom and upper channels were α_b = 3.52, and, α_u = 7.21 respectively under a total pumping power of 0.1 W. It should be noted that the total height of the heat sink in Hung et al. [6] was fixed, while the height of the bottom microchannels was varied with the changes of channel number, bottom channel aspect ratio or channel width ratio. This result demonstrates that the optimal geometric sizes of DL-MCHS are highly dependent on the constraint conditions used in the optimization work.

Comparing the results of cases of N = 100 with N = 71, N = 120 with "N = 84", and N = 133 with N = 94, it is found that the cases of W_{ch} = 50 μm provide better overall thermal performance over the cases of W_{ch} = 70 μm with same width ratio of β. Therefore, the performance of DL-MCHS with microchannel width of 40 μm (α = 6.25) and channel number of 125 (β = 1.0) and 153 (β = 0.63) are further simulated, without considering the case of β = 0.50 again. The numerical results are shown in Figs. 14–16 show. Fig. 14 shows that the thermal resistance decreases with increase of channel number and decrease less and less when inlet velocity increases. Fig. 15 shows that with a given pumping power, the case of N = 125 (β = 1.0) exhibits lower thermal resistance than that of the case of N = 153 (β = 0.63). Fig. 16 shows that the case of N = 125 (β = 1.0) exhibits lower temperature rise along heated surface in higher inlet velocity than that of case of N = 153 (β = 0.63). This demonstrates again the optimal width ratio of β is not 0.5, even not 0.6–0.7, should be much higher for the DL-MCHS with microchannel width of 40 μm (α = 6.25). Thus, it is concluded from the results of this section that the optimal width ratio β (channel number N) of DL-MCHS is dependent on the microchannel width or aspect ratio.

4.3. Effect of microchannel aspect ratio on the performance of DL-MCHS

To estimate the effect of microchannel aspect ratio on the overall performance of DL-MCHS, the performances of the three better cases with different upper/lower microchannel widths of 70 (α = 3.57, N = 84), 50 (α = 5, N = 120) and 40 μm (α = 6.25, N = 125) are compared, as shown in Figs. 17–19. It is found from

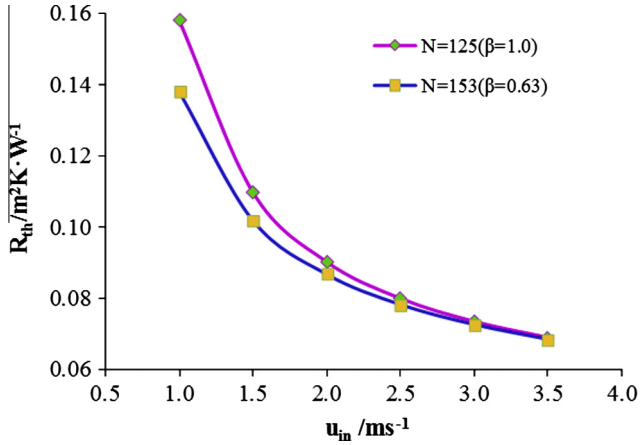

Fig. 14. Comparison of thermal resistance vs. inlet velocity between the two cases of W_{ch} = 40 μm.

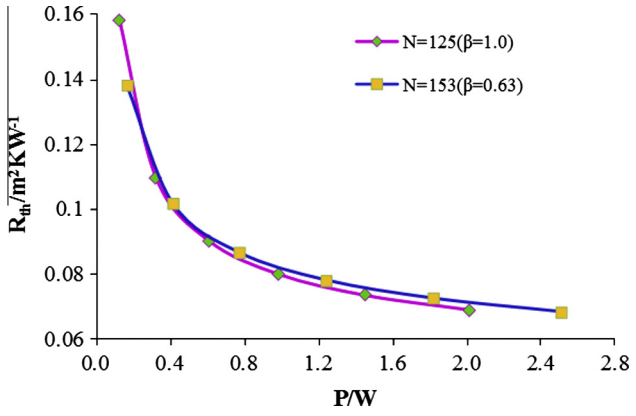

Fig. 15. Comparison of thermal resistance vs. pumping power between the two cases of W_{ch} = 40 μm.

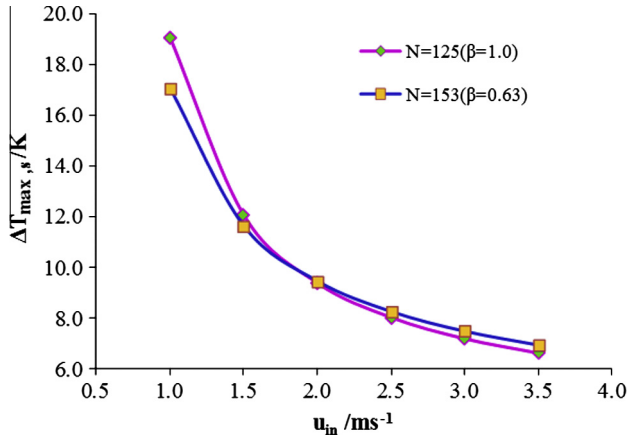

Fig. 16. Comparison of temperature rise vs. inlet velocity between the two cases of W_{ch} = 40 μm.

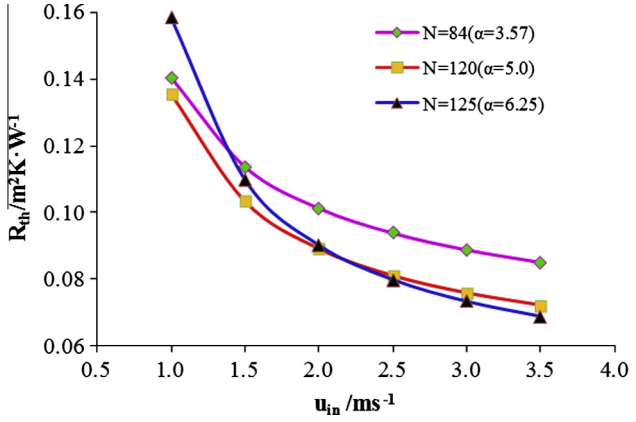

Fig. 17. Effect of aspect ratio on thermal resistance.

Fig. 17 that the case of N = 120 (α = 5) contributes lower thermal resistance than the case of N = 84 (α = 3.57) in the whole range of computational inlet velocity. While the case of N = 125 (α = 6.25) exhibits higher thermal resistance in lower inlet velocity range, and lower thermal resistance in higher inlet velocity range than the case of N = 120 (α = 5). The variations of thermal resistance along with pumping power of the three cases are compared in Fig. 18. It shows that the case of N = 120 (α = 5) always contributes lower thermal resistance than the case of N = 125 (α = 6.25) at a

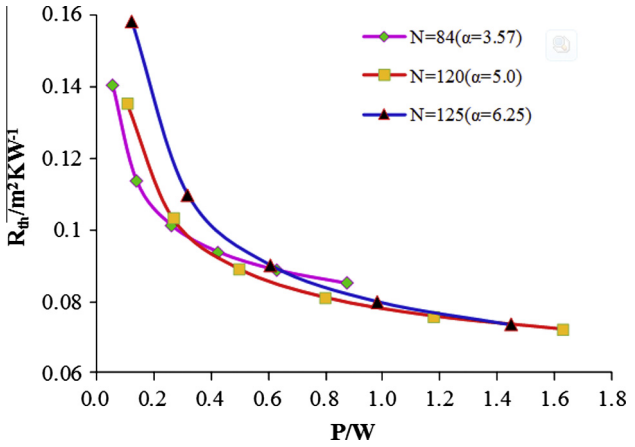

Fig. 18. Comparison of thermal resistance vs. pumping power between cases of different aspect ratio.

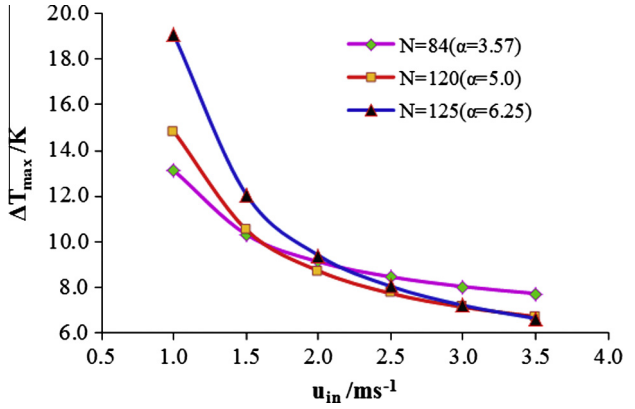

Fig. 19. Effect of aspect ratio on temperature rise.

given pumping power. While the case of N = 84 (α = 3.57) performs better than the case of N = 120 (α = 5) in lower pumping power (lower inlet velocity). From the point of the uniformity of temperature distribution, the case of N = 120 (α = 5) always exhibits lower temperature rise than the case of N = 125 (α = 6.25) in the whole computational range, as shown in Fig. 19. While the case of N = 84 (α = 3.57) presents lower temperature rise than the two other cases in lower inlet velocity conditions. It is suggested that when pumping power is given less than 0.25 W, the case of N = 84 (α = 3.57, β = 0.69) may provide better overall performance than the other two ones. However, when pumping power is given between 0.25 and 1.3 W, the case of N = 120 (α = 5.0, β = 0.66) performs better. These results show that the effectiveness of increasing microchannel aspect ratio (decreasing microchannel width) on improving the overall performance of DL-MCHS is dependent on the pumping power provided. DL-MCHS with higher aspect ratio may have good overall performance if higher pumping power is provided. This suggest that in the design of DL-MCHS, the microchannel aspect ratio and width ratio should match the provided pumping power, so as to be able to develop DL-MCHS with lower thermal resistance and more uniform temperature distribution.

4.4. Effect of velocity ratio on the performance of DL-MCHS

In above simulation, upper and bottom channels are assigned with same inlet velocity. It is found that the coolant in upper channels always have lower temperature rise from inlet to outlet than that in bottom channels. This results in higher viscosity of coolant

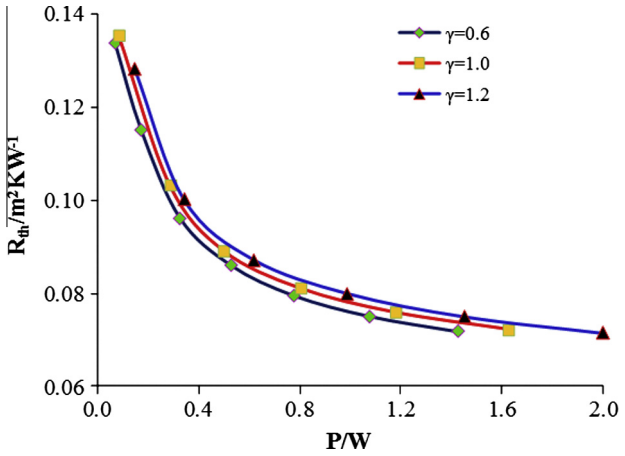

Fig. 20. Comparison of thermal resistance vs. inlet velocity at different velocity ratio for case of $N = 120$.

in upper channels due to lower coolant temperature. Thus, the pressure drop in upper channels is always higher than that in bottom channels. In this section, it is tried to assign different inlet velocity to the upper and bottom channels to investigate the effect of velocity ratio of γ (defined as the ratio of upper channel inlet velocity to bottom channel inlet velocity, $=u_{in,u}/u_{in,b}$) on the performance of DL-MCHS. The case of $N = 120$ ($W_{ch} = 50$ μm, $\alpha = 5.0$, $\beta = 0.66$) suggested as the better one in the above results is selected to explore this effect. γ can be 0.6, 1.0 and 1.2. The situation of $\gamma = 1.0$ is just the above simulation condition. Fig. 20 shows the variation of thermal resistance of this case vs. pumping power consumed at different velocity ratio. It is found that with a given pumping power, decreasing the velocity ratio of γ brings about the decrease of the thermal resistance of this heat sink. This implies that when we control the inlet velocity of upper channels to be smaller than that of bottom channels, we may obtain lower thermal resistance at a given pumping power. This benefit is especially obvious when the given pumping power is lower. This is because the decrease of the inlet velocity in the upper channels

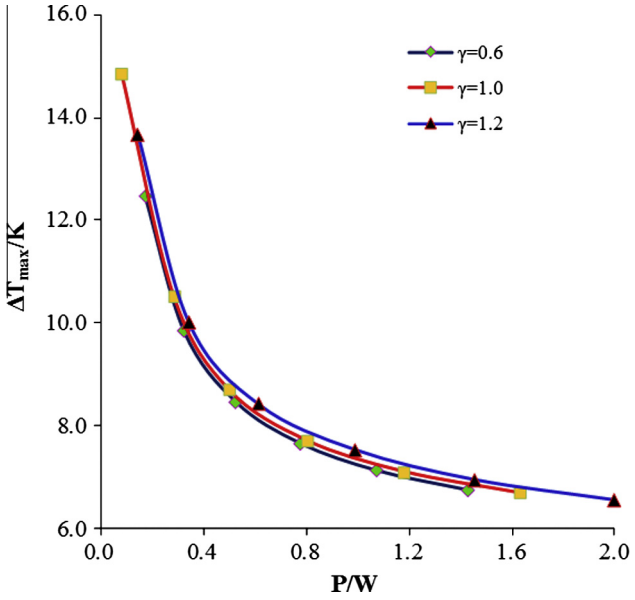

Fig. 21. Comparison of temperature rise vs. pumping power at different velocity ratio for case of $N = 120$.

can greatly reduce the pressure drop even if the coolant in the upper channels may still have a higher viscosity. Reduced pressure drop and lower volume rate in the upper microchannel lead to a decrease of total pumping power. Fig. 21 shows the variation of temperature rise of this case vs. pumping power consumed at different velocity ratio. It is also found that with a given pumping power, the decrease of γ can decrease the temperature rise and improve the uniformity of temperature distribution on the heated surface of DL-MCHS. It is suggested that for DL-MCHS with equal depth of upper and bottom channel, adjusting the inlet velocity of upper channels to be smaller than that of bottom channels may improve the overall performance of DL-MCHS at a given pumping power.

5. Conclusions

Electronic cooling remains a challenging subject that needs more work due to the high heat flux needed to be removed. Double-layered microchannel heat sinks are expected to meet the ever increasing heat load of future generation electronic devices by reducing the thermal resistance and improving the uniformity of temperature distribution on the base surface of heat sink. The present paper numerically investigated the effects of channel number (width ratio), aspect ratio and velocity ratio on the overall thermal performance of DL-MCHS with given bulk sizes ($L \times W \times h$) and heat removal required. The following conclusions are reached.

(1) When microchannel width is fixed, decreasing width ratio (increasing microchannel number) does not always work in reducing the thermal resistance and improving the uniformity of temperature distribution on the base surface of DL-MCHS at a given pumping power. In this study, the better width ratio for the cases with microchannel width of 50 and 70 μm should be 0.6–0.7. While for the case with microchannel width of 40 μm, the width ratio should be increased because too small width ratio (too large microchannel number) may result in large pumping power consumed and slight decrease of thermal resistance. This means the optimal DL-MCHS width ratio is dependent on the aspect ratio of microchannel.
(2) The effectiveness of increasing aspect ratio (decreasing microchannel width) on improving the overall performance of DL-MCHS relies on the pumping power provided. DL-MCHS with higher aspect ratio (small microchannel width) and larger channel number (small width ratio) is suited to the situation when higher pumping power is provided. Thus in the design of DL-MCHS, the microchannel aspect ratio and channel number should match the pumping power provided.
(3) Compared with the situation with identical inlet velocity being assigned to the bottom and upper microchannels, adjusting the inlet velocity of upper channels to be smaller than that of bottom channels may improve the overall performance of DL-MCHS at a given pumping power. This benefit is especially obvious when the given pumping power is lower. This strategy could be tried in the application of DL-MCHS.

Acknowledgement

This work is supported by the "National Natural Science Foundation of China" (Grant No. 51276146) and Program for Changjiang Scholars and Innovative Research Team in University (PCSIRT, IRT1280).

References

[1] Vafai K, Zhu L. Analysis of two-layered micro-channel heat sink concept in electronic cooling. Int J Heat Mass Transfer 1999;42:2287–97.

[2] Wei X, Joshi. Stacked microchannel heat sinks for liquid cooling of microelectronic components. J Electron Packag 2004;126:60–6.

[3] Wei X, Joshi Y, Patterson MK. Experimental and numerical study of a stacked microchannel heat sink for liquid cooling of microelectronic devices. J Heat Transfer 2007;129:1432–44.

[4] Levac M, Soliman H, Ormiston S. Three-dimensional analysis of fluid flow and heat transfer in single and two-layered micro-channel heat sinks. Heat Mass Transfer 2011;47:1375–83.

[5] Hung TC, Yan WM, Li WP. Analysis of heat transfer characteristics of double-layered microchannel heat sink. Int J Heat Mass Transfer 2012;55:3090–9.

[6] Hung TC, Yan WM, Li WP, Huang YX. Optimal design of geometric parameters of double-layered microchannel heat sinks. Int J Heat Mass Transfer 2012;55:3262–72.

[7] Hung TC, Sheu TS, Yan WM. Optimal thermal design of microchannel heat sinks with different geometric configurations. Int Commun Heat Mass Transfer 2012;39:1572–7.

[8] Hung TC, Yan WM. Enhancement of thermal performance in double-layered microchannel heat sink with nanofluids. Int J Heat Mass Transfer 2012;55:3225–38.

[9] Xie GN, Liu YQ, Zhang WL, Sunden B. Computational study and optimization of laminar heat transfer and pressure loss of double-layer microchannels for chip liquid cooling. ASME J Therm Sci Eng Appl 2013;5:011004.

[10] Li J, Peterson GP. 3-Dimensional numerical optimization of silicon-based high performance parallel microchannel heat sink with liquid flow. Int J Heat Mass Transfer 2007;50:2895–904.